

Note

# Size, albedo, and taxonomic type of potential spacecraft target Asteroid (10302) 1989 ML

Michael Mueller<sup>a,\*</sup>, Alan W. Harris<sup>a</sup>, Alan Fitzsimmons<sup>b</sup>

<sup>a</sup> DLR Institute of Planetary Research, Rutherfordstraße 2, 12489 Berlin, Germany

<sup>b</sup> Astrophysics Research Centre, Queen's University Belfast, BT7 1NN, UK

Received 29 September 2006; revised 18 December 2006

Available online 30 January 2007

## Abstract

The Amor-type near-Earth Asteroid (10302) 1989 ML has an “Earth-like” orbit (period 1.44 yr, eccentricity 0.14, inclination 4.4°), therefore the energy required to reach it from the Earth is relatively small making it a very attractive target for rendezvous missions. We have observed 1989 ML in the thermal–infrared using the Spitzer Space Telescope, and compared these data with optical and near-infrared observations. The Spitzer results imply a diameter of  $0.28 \pm 0.05$  km and a geometric albedo of  $0.37 \pm 0.15$ ; together with the reflectance spectrum they are consistent with the relatively rare E classification.

© 2007 Elsevier Inc. All rights reserved.

**Keywords:** Asteroids; Infrared observations; Near-Earth objects; Spectrophotometry

## 1. Introduction

The most accessible asteroids for rendezvous missions are those with orbits similar to that of the Earth. Indeed, some near-Earth asteroids (NEAs) are easier to reach than the Moon. The energy and flight time required to reach the NEA (10302) 1989 ML are relatively small, comparable to those for the Hayabusa target (25143) Itokawa (Perozzi et al., 2001; Christou, 2003; Binzel et al., 2004), making it a very attractive spacecraft target for rendezvous missions. 1989 ML has been considered as a possible target for both the Japanese Hayabusa and the European Don Quijote missions (see, for example, Binzel et al., 2001 and <http://www.esa.int/SPECIALS/NEO/>); at the time of writing further missions to NEAs are being planned in Japan, Europe, and the USA, for which 1989 ML may be considered as a target. *However, a serious and urgent problem for mission planning is the lack of information on the physical properties of this asteroid.*

Preliminary optical lightcurve measurements by Abe et al. (2000) and Weissman et al. (1999) suggest the peak-to-peak

amplitude is about 1 mag, corresponding to a very elongated shape. Weissman et al. (1999) report a rotation period near 19 h. However, according to Abe et al. (2000), ~32 h is also possible. This long-period high-amplitude lightcurve has limited the accuracy of determinations of the absolute optical magnitude  $H$  (see Bowell et al., 1989 for details of the  $H$ ,  $G$  magnitude system): Abe et al. (2000) report  $H = 19.7$  (assuming  $G = 0.15$ ); NEODys (as of 2006/12/08) reports  $H = 19.39$  ( $G = 0.15$ ); Weissman et al. (1999) report an absolute magnitude in the R band of  $H_R = 19.14$ , which implies  $H = 19.51$  using  $V-R = 0.37 \pm 0.03$  (see Section 3.2). Since published  $H$  values for NEAs are notoriously unreliable, we adopt the average value of  $H = 19.5$  with a conservative uncertainty of  $\pm 0.3$ .

Binzel et al. (2001) report a neutral Xc-type spectrum at optical wavelengths, implying that 1989 ML belongs to one of the E, M, or P spectrally degenerate classes. E-type asteroids have a high geometric albedo  $p_v$  ( $0.3 < p_v < 0.6$ ) and may be related to enstatite achondrite meteorites; M-type asteroids have moderate albedos around 0.1–0.2 and some are probably related to metallic meteorites; P-type asteroids have very low albedos ( $p_v < 0.1$ ) and appear to be organic-rich, similar to carbonaceous chondrites (see, e.g., Clark et al., 2004a, 2004b).

\* Corresponding author. Fax: +49 30 67055 340.

E-mail address: [michael.mueller@dlr.de](mailto:michael.mueller@dlr.de) (M. Mueller).

Determination of the albedo of an X-type asteroid is therefore very important for constraining its composition.

The sizes and albedos of asteroids can be determined from optical and thermal-infrared observations, together with appropriate thermal modeling (e.g., [Lebofsky and Spencer, 1989](#); [Harris and Lagerros, 2002](#) and references therein). The diameter  $D$ , the geometric albedo  $p_v$ , and the absolute optical magnitude  $H$  are related by ([Fowler and Chillemi, 1992](#)):

$$p_v = 10^{-H/2.5} (1329 \text{ km}/D)^2. \quad (1)$$

We observed 1989 ML in the thermal-infrared using the Infrared Array Camera IRAC ([Fazio et al., 2004](#)) onboard the Spitzer Space Telescope, and in the optical using the 2.0-m Faulkes Telescope North. We employed the Near-Earth-Asteroid Thermal Model (NEATM) ([Harris, 1998](#)) to derive the effective diameter from the Spitzer data. NEATM fits require measurements of the lightcurve-averaged thermal continuum at two or more wavelengths. The diameter and the model parameter  $\eta$  are varied to obtain the best fit of the model continuum to the observed fluxes. Varying  $\eta$  varies the effective color temperature of the model thermal continuum, which allows for the combined effects of thermal inertia, beaming due to roughness, and solar phase angle; note that our Spitzer observations took place at a phase angle of  $52.3^\circ$ . For more detailed discussions of the NEATM see [Harris \(1998\)](#), [Delbó and Harris \(2002\)](#), [Harris and Lagerros \(2002\)](#), and [Delbó et al. \(2003\)](#), and references therein.

## 2. Observations and data reduction

### 2.1. Spitzer observations

1989 ML was observed on 2006 June 2 and 3 with the infrared imaging camera IRAC. IRAC has four filter passbands, referred to as channels 1–4 in the following, with effective wavelengths of 3.550, 4.493, 5.731, and 7.872  $\mu\text{m}$ , respectively, and FWHM of more than 20% (cf. the IRAC data handbook: <http://ssc.spitzer.caltech.edu/irac/dh/>).

We observed the asteroid six times, each observation providing nearly simultaneous photometry in all 4 IRAC channels with five dither positions, of 30 s integration time each, per field-of-view. The observation time in each case was about 12 min, including dead times for telescope slewing and settling, which is significantly shorter than the asteroid rotation period (see Section 1). There was a time gap of  $\sim 3.2$  h between consecutive observations, corresponding to  $\sim 60^\circ$  in rotational phase assuming the nominal rotation period of 19 h ([Weissman et al., 1999](#)). The observing geometry did not change significantly during our observations: the heliocentric distance was 1.270 AU, the distance to Spitzer was 0.891 AU, and the solar phase angle,  $\alpha$ , was  $52.3^\circ$  (source: JPL Horizons System; all values are constant during our Spitzer observations to  $\pm 2$  in the last quoted digit or better).

Correction for most instrument artifacts (including dark current and flatfield) and absolute flux calibration against a set of standard stars (see [Fazio et al., 2004](#)) was performed by the automated IRAC data reduction pipeline hosted by the

Table 1  
Flux densities derived from Spitzer IRAC observations

JD-2453889.0	Flux ( $\mu\text{Jy}$ )	$\sigma$ flux ( $\mu\text{Jy}$ )
0.47827	126 (122)	19 (18)
0.60011	49 (47)	16 (15)
0.75043	115 (112)	23 (22)
0.86787	188 (182)	17 (16)
1.01833	91 (89)	21 (20)
Central wavelength ( $\mu\text{m}$ )	Flux ( $\mu\text{Jy}$ )	$\sigma$ flux ( $\mu\text{Jy}$ )
3.550	4.14 (4.14)	0.77 (0.77)
4.493	4.1 (3.8)	1.3 (1.2)
5.731	21.7 (20.3)	7.3 (6.8)
7.872	111.3 (108)	17.7 (18)

*Notes.* Above: time-resolved channel-4 fluxes (7.872  $\mu\text{m}$ ). Below: average fluxes for all four IRAC channels derived from stacking observations 1–5. Flux values in parentheses are color corrected (see Section 3.1). Times refer to the beginning of the observations and are not light-time corrected.

Spitzer Science Center, resulting in ‘basic calibrated data’ (BCD) image frames. We used the software package MOPEX (see [Makovoz and Khan, 2005](#)) to mosaic the BCD images, i.e., to co-add them in the asteroid rest frame, rejecting non-co-moving sources such as background stars or cosmic ray hits. The asteroid flux was derived from the resulting mosaic images using standard synthetic aperture photometry procedures. A discussion of the color corrections to the derived flux densities is given in Section 3.1. The mosaics for observations 1–5 display clear asteroid signals at the predicted positions, but observation 6 failed, because the target asteroid was within  $2''$  of a background star of comparable brightness. Also, data from observation 4 are compromised by the presence of a faint background source, which can be neglected for IRAC channels 3 and 4 but has comparable flux to that of the asteroid at shorter wavelengths.

The highest signal-to-noise ratio is obtained in IRAC channel 4, from which photometry can be extracted for observations 1 through 5, yielding a coarse thermal lightcurve. For all channels we stacked images from observations 1–5 and derived an average flux value from the resulting mosaic images. The flux values are listed in [Table 1](#).

### 2.2. Optical observations

In order to provide further photometric data on 1989 ML, it was observed on 2006 January 4.5 UT using the 2.0-m Faulkes Telescope North at the Haleakala observatory on Maui, Hawaii, at a solar phase angle around  $1.1^\circ$ . BVRI imaging was obtained with the DILCAM CCD camera, a clone of the RATCAM instrument ([Steele, 2001](#)). The telescope was tracked at sidereal rates, so exposure times were limited to 40 s to ensure that trailing of the target did not occur. The NEA was imaged using the sequence R–B–R–V–R–I–R . . . , to allow interpolation of the colors relative to R over the lightcurve. Unfortunately the observations spanned only 2.5 h, and so did not allow further refinement of the spin period. Observations of standard stars ([Landolt, 1992](#)) were obtained during this period to allow photometric calibration and hence provide apparent magnitudes and colors.

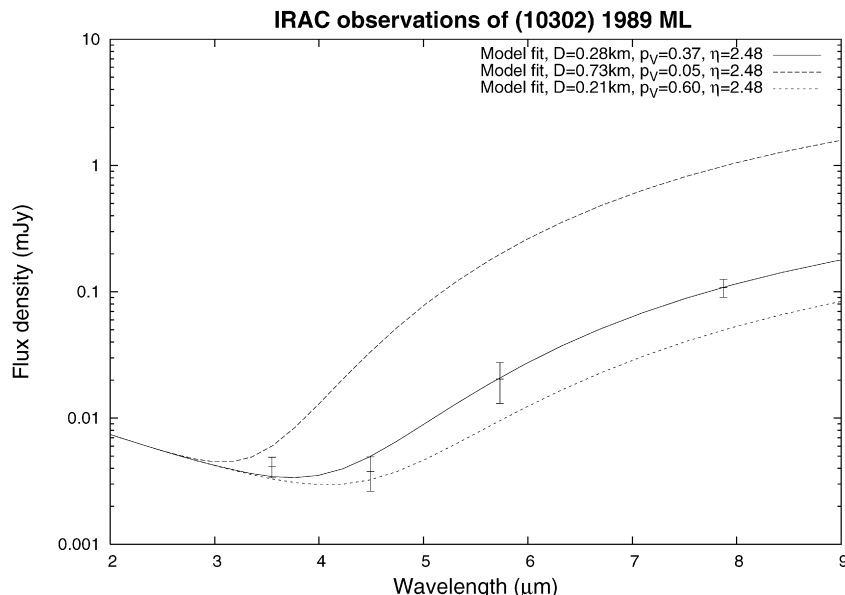


Fig. 1. Model fits to the photometric data given in Table 1. Both reflected sunlight and thermal emission are modeled (cf. text). The thermal contributions to channels 3 and 4 (wavelengths 5.7 and 7.9  $\mu\text{m}$ ) are fitted using NEATM; the reflected sunlight is extrapolated from the predicted  $V$  magnitude assuming a relative reflectance of 1.2 (cf. text and Fig. 2). An albedo of  $p_v = 0.05$ , which would be typical for P-type asteroids, is clearly incompatible with the data (dashed line).

### 3. Results

#### 3.1. Spitzer results

Our time-resolved channel-4 data (7.872  $\mu\text{m}$ ) given in Table 1 (upper part) are consistent with a high-amplitude long-period lightcurve (see Section 1). Sinusoidal double-peaked lightcurves corresponding to the two possible rotation periods of 19 and 32 h fit the data well. The average flux levels of the two fitted lightcurves are consistent with one another and with the flux value obtained from stacking images from observations 1–5 (cf. Table 1, lower part). Agreement is to within a few percent, a negligible difference compared to the statistical flux uncertainty. We cannot further constrain the rotation properties from our Spitzer data, but conclude that for all IRAC channels the flux values obtained from stacking observations 1–5 are good proxies to the lightcurve average flux level.

IRAC is a broad-band photometer, so the derived flux values must be color corrected, taking account of the detector spectral response and the asteroid spectral shape. Color correction factors for several target spectra are tabulated in the IRAC data handbook, p. 48 (<http://ssc.spitzer.caltech.edu/irac/dh/>). A routine was developed to calculate color-correction factors for several model spectra, including NEATM spectra (using the IRAC spectral detector responses provided online by the Spitzer Science Center). We verified that our software reproduces the correction factors provided in the data handbook. Due to their different spectral shapes, different color corrections apply to the thermally emitted flux component and to reflected sunlight; color corrections to the latter are negligible.

We estimated the amount of reflected sunlight in channels 1–4 assuming a solar black body temperature of 5800 K and a relative reflectance of  $\sim 1.2$  between 3.6  $\mu\text{m}$  and the  $V$  band (cf. Fig. 2). Reflected sunlight was found to contribute virtually

all the measured flux in channel 1, only negligible amounts in channel 4, and  $\sim 1 \mu\text{Jy}$  in channel 3 ( $\sim 5\%$  of the measured flux). The relative contributions to the channel-2 flux cannot be easily determined.

We fitted NEATM to the thermal flux values from channels 3 and 4 and calculated color-correction factors using the model parameters (diameter,  $p_v$ , and  $\eta$ ) derived. We repeated this procedure with color-corrected thermal fluxes, after which the procedure was seen to have converged; a second iteration brought about changes significantly below the 1% level. The resulting model spectrum with the observational data overlaid is shown in Fig. 1.

The best-fit parameters are: diameter  $D = 0.276$  km, albedo  $p_v = 0.37$ , and  $\eta = 2.48$ . Color-corrected fluxes were obtained by dividing the thermal contributions to fluxes by 1.129 (channel 2), 1.070 (channel 4), and 1.034 (channel 4). Uncertainties in  $D$ ,  $p_v$  and  $\eta$  were estimated using a Monte-Carlo analysis. To this end, we generated a random set of synthetic thermal flux values at the channel-3 and channel-4 wavelengths, normally distributed around the measured values, and fitted them with NEATM. We rejected unrealistic results with  $\eta > 3$  or  $p_v > 0.7$ . The remaining sample of 15,000 results gave  $D = 0.246 \pm 0.037$  km,  $p_v = 0.46 \pm 0.13$ , and  $\eta = 2.23 \pm 0.44$  ( $1\sigma$  standard deviations—note, however, that the distribution of resulting model parameters is highly non-Gaussian). We adopt the relative uncertainties from this simulation for our best-fit results stated above, yielding:  $D = 0.276 \pm 0.041$  km,  $p_v = 0.37 \pm 0.11$ , and  $\eta = 2.48 \pm 0.49$ . The uncertainty in our adopted value for  $H$  ( $19.5 \pm 0.3$ ) contributes an additional 30% to the albedo error (added in quadrature) so  $p_v = 0.37 \pm 0.15$ . This albedo is suggestive of an E classification. P types, for which  $p_v$  should not exceed 0.1 (cf. Section 1), would appear to be ruled out (see also Fig. 1). We note that in addition to the statistical errors there is a systematic modeling uncertainty that

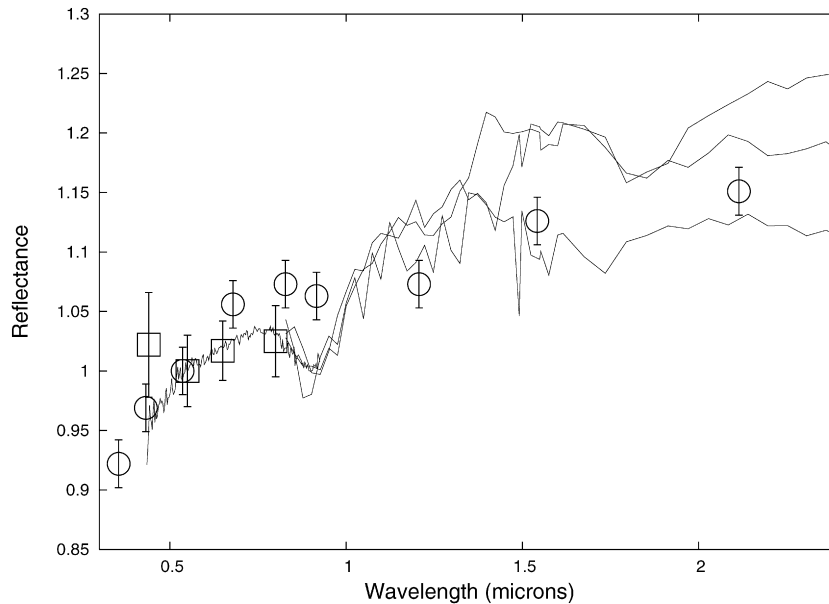


Fig. 2. Comparison of photometry of 1989 ML with spectra of (44) Nysa. Square symbols represent optical colors given in this paper; circles represent the optical and near-infrared data reported by Hiroi et al. (2000). The continuous line covering 0.4–1.0  $\mu\text{m}$  is the spectrum of (44) Nysa from the SMASS II dataset by Bus and Binzel (2003). The three continuous lines extending from 0.9 to 2.5  $\mu\text{m}$  are individual spectra of (44) Nysa from the 52-color asteroid survey (Bell et al., 1995). Optical data were normalized to a wavelength of 0.55  $\mu\text{m}$ . The near-infrared spectra were scaled to match the optical spectrum near 0.95  $\mu\text{m}$ .

increases with solar phase angle and thermal inertia (see Harris, 2006), but in the sense of underestimating  $p_v$ . So the systematic uncertainty in the NEATM results in this case would tend to increase  $p_v$  above the value of 0.37 derived here.

The derived  $\eta$  value of  $2.5 \pm 0.5$  is rather high for a solar phase angle of  $52^\circ$  (Delbó et al., 2003) and is consistent with a high surface thermal inertia, corresponding to a lack of thermally insulating dust or regolith. Better spectral coverage and a thermophysical model would be required to derive conclusive statements about surface thermal properties.

### 3.2. Optical and near-infrared data

Our optical photometry revealed the following colors:  $(B-V) = 0.63 \pm 0.05$ ,  $(V-R) = 0.37 \pm 0.03$ ,  $(V-I) = 0.74 \pm 0.03$ . These colors are consistent with those reported by Abe et al. (2000) but have significantly smaller uncertainties. ECAS and near-IR (JHK) photometry of 1989 ML has also been obtained by D. Tholen and is reported in Hiroi et al. (2000). Taken together, these datasets show that the optical/NIR colors are redder than solar, with a spectral break to a less steep slope occurring around a wavelength of  $\sim 0.7 \mu\text{m}$ ; they are consistent with the optical spectrum reported by Binzel et al. (2001).

To investigate the possible taxonomic types we compared these data with spectra of previously classified asteroids from the SMASS II (Bus and Binzel, 2003) and the 52-color catalogues (Bell et al., 1995). Fig. 2 shows the optical and IR photometry compared to 52-color data of the E-type Asteroid (44) Nysa, demonstrating a clear correspondence. However, the colors of the E-type Asteroids (64) Angelina and (3101) Eger are inconsistent with the 1989 ML colors. Clark et al. (2004a) have shown that Nysa-type spectra are consistent with a sili-

cate mineralogy higher in iron than the mineral enstatite, while Angelina-type spectra are consistent with sulfide-bearing silicates. Interestingly, although E, M, and P types are spectrally degenerate in the optical, we were not able to obtain similar agreement with 52-color data of the M types (16) Psyche and (216) Kleopatra, nor the P types (65) Cybele and (153) Hilda. Therefore we conclude that the available optical-NIR data support a relatively Fe-enriched E-type classification, in agreement with our Spitzer data.

## 4. Summary

On the basis of thermal-infrared photometric observations of near-Earth Asteroid (10302) 1989 ML using the IRAC camera onboard the Spitzer Space Telescope we have determined its effective diameter to be  $0.28 \pm 0.05 \text{ km}$  and its geometric albedo  $p_v$  to be  $0.37 \pm 0.15$ . This high albedo is incompatible with a P-type classification, is only marginally consistent with an M-type classification, but is fully consistent with an E-type classification. The available optical and near-infrared data also favor E type. Taken together, we conclude that the available data suggest an E classification for (10302) 1989 ML—note that only 4 E-type near-Earth asteroids were known so far (Clark et al., 2004a).

## Acknowledgments

This work is based on observations made with the Spitzer Space Telescope, which is operated by the Jet Propulsion Laboratory, California Institute of Technology under a contract with NASA. The comments and suggestions of the referees, Beth Clark and Marco Delbó, are gratefully acknowledged.

## References

- Abe, M., Sato, I., Araki, H., 2000. Lightcurve and color of near-earth-asteroid 1989ML. *Adv. Space Res.* 25, 269–272.
- Bell, J.F., Owensby, P.D., Hawke, B.R., Brown, R.H., Cruikshank, D., Hartmann, W.K., 1995. 52-color asteroid survey. EAR-A-RDR-3-52COLOR-V2.1. NASA Planetary Data System.
- Binzel, R.P., Harris, A.W., Bus, S.J., Burbine, T.H., 2001. Spectral properties of near-Earth objects: Palomar and IRTF results for 48 objects including spacecraft targets (9969) Braille and (10302) 1989 ML. *Icarus* 151, 139–149.
- Binzel, R.P., Perozzi, E., Rivkin, A.S., Rossi, A., Harris, A.W., Bus, S.J., Valsecchi, G.B., Slivan, S.M., 2004. Dynamical and compositional assessment of near-Earth object mission targets. *Meteorit. Planet. Sci.* 39, 351–366.
- Bowell, E., Hapke, B., Domingue, D., Lumme, K., Peltoniemi, J., Harris, A.W., 1989. Application of photometric models to asteroids. In: Binzel, R.P., Gehrels, T., Matthews, M.S. (Eds.), *Asteroids II*. Univ. of Arizona Press, Tucson, pp. 524–556.
- Bus, S., Binzel, R.P., 2003. Small main-belt asteroid spectroscopic survey, phase II. EAR-A-10028-4-SBN0001/SMASII-V1.0. NASA Planetary Data System.
- Christou, A.A., 2003. The statistics of flight opportunities to accessible near-Earth asteroids. *Planet. Space Sci.* 51, 221–231.
- Clark, B.E., Bus, S.J., Rivkin, A.S., McConnochie, T., Sanders, J., Shah, S., Hiroi, T., Shepard, M., 2004a. E-type asteroid spectroscopy and compositional modeling. *J. Geophys. Res.* 109 (E2), doi:10.1029/2003JE002200. E02001.
- Clark, B.E., Bus, S.J., Rivkin, A.S., Shepard, M.K., Shah, S., 2004b. Spectroscopy of X-type asteroids. *Astron. J.* 128, 3070–3081.
- Delbó, M., Harris, A.W., 2002. Physical properties of near-Earth asteroids from thermal infrared observations and thermal modeling. *Meteorit. Planet. Sci.* 37, 1929–1936.
- Delbó, M., Harris, A.W., Binzel, R.P., Pravec, P., Davies, J.K., 2003. Keck observations of near-Earth asteroids in the thermal infrared. *Icarus* 166, 116–130.
- Fazio, G.G., and 64 colleagues, 2004. The Infrared Array Camera (IRAC) for the Spitzer Space Telescope. *Astrophys. J. Suppl.* 154, 10–17.
- Fowler, J.W., Chillemi, J.R., 1992. IRAS data processing. In: Tedesco, E.F. (Ed.), *The IRAS Minor Planet Survey*. Tech. Report PL-TR-92-2049. Phillips Laboratory, Hanscom Air Force Base, MA, pp. 17–43.
- Harris, A.W., 1998. A thermal model for near-Earth asteroids. *Icarus* 131, 291–301.
- Harris, A.W., 2006. The surface properties of small asteroids from thermal-infrared observations. In: Lazzaro, D., Ferraz-Mello, S., Fernández, J.A. (Eds.), *Proc. of IAU Symposium*, vol. 229. Cambridge Univ. Press, Cambridge, pp. 449–463.
- Harris, A.W., Lagerros, J.S.V., 2002. Asteroids in the thermal infrared. In: Bottke, W.F., Paolicchi, P., Binzel, R.P., Cellino, A. (Eds.), *Asteroids III*. Univ. of Arizona Press, Tucson, pp. 205–218.
- Hiroi, T., Zolensky, E.M., Lipschutz, E.M., 2000. Possible meteorite analogs for Asteroid 1989 ML—Target of MUSES-C asteroid sample return mission. *Antarctic Meteorit.* 25, 14–15.
- Landolt, A.U., 1992. UBVRI photometric standard stars in the magnitude range 11.5–16.0 around the celestial equator. *Astron. J.* 104, 340–371, 436–491.
- Lebofsky, L.A., Spencer, J.R., 1989. Radiometry and thermal modeling of asteroids. In: Binzel, R.P., Gehrels, T., Matthews, M.S. (Eds.), *Asteroids II*. Univ. of Arizona Press, Tucson, pp. 128–147.
- Makovoz, D., Khan, I., 2005. Mosaicking with MOPEX. In: Shopbell, P.L., Britton, M.C., Ebert, R. (Eds.), *Astronomical Data Analysis Software and Systems, XIV ASP Conf. Ser.*, vol. 347. ASP, San Francisco, pp. 81–85.
- Perozzi, E., Rossi, A., Valsecchi, G.B., 2001. Basic targeting strategies for rendezvous and flyby missions to the near-Earth asteroids. *Planet. Space Sci.* 49, 3–22.
- Steele, I.A., 2001. The Liverpool Telescope. *Astron. Nachr.* 332, 307–310.
- Weissman, P., Doressoundiram, A., Hicks, M., Chamberlin, A., Sykes, M., Larson, S., Hergenrother, C., 1999. CCD photometry of comet and asteroid targets of spacecraft missions. *Bull. Am. Astron. Soc.* 31. Abstract #30.03.